Development of Crosslinked Methylcellulose Hydrogels for Soft Tissue Augmentation using an Ammonium Persulfate-Ascorbic Acid Redox System

Gittel T. Gold[1], Devika M. Varma[1], Peter J. Taub[2], and Steven B. Nicoll[1,*]

[1]Department of Biomedical Engineering

The City College of New York, New York, NY

[2]Division of Plastic and Reconstructive Surgery

The Mount Sinai Medical Center, New York, NY

* Corresponding Author:

Steven B. Nicoll, Ph.D.

Associate Professor

Department of Biomedical Engineering

Grove School of Engineering

The City College of New York

Steinman Hall, Room 401

160 Convent Avenue

New York, NY 10031

Tel: 212-650-6237

Fax: 212-650-6727

Email: snicoll@ccny.cuny.edu

Abstract

Hydrogels composed of methylcellulose are candidate materials for soft tissue reconstruction. Although photocrosslinked methylcellulose hydrogels have shown promise for such applications, gels crosslinked using reduction-oxidation (redox) initiators may be more clinically viable. In this study, methylcellulose modified with functional methacrylate groups was polymerized using an ammonium persulfate (APS)-ascorbic acid (AA) redox initiation system to produce injectable hydrogels with tunable properties. By varying macromer concentration from 2% to 4% (w/v), the equilibrium moduli of the hydrogels ranged from 1.47 ± 0.33 to 5.31 ± 0.71 kPa, on par with human adipose tissue. Gelation time was found to conform to the ISO standard for injectable materials. Cellulase treatment resulted in complete degradation of the hydrogels within 24 hours, providing a reversible corrective feature. Co-culture with human dermal fibroblasts confirmed the cytocompatibility of the gels based on DNA measurements and Live/Dead imaging. Taken together, this evidence indicates that APS-AA redox-polymerized methylcellulose hydrogels possess properties beneficial for use as soft tissue fillers.

1. Introduction

Soft tissue fillers that are cytocompatible, injectable (Drury & Mooney, 2003; Page, Harmata, & Guelcher, 2013) and long-lasting are needed to treat deficits resulting from tumor resection (Shpaisman, Sheihet, Bushman, Winters, & Kohn, 2012), lipoatrophy (Barton, Engelhard, & Conant, 2006; Jones, 2005; Kadouch, van Rozelaar, Karim, & Hoekzema, 2013; Negredo et al., 2006), congenital anomalies and trauma. The majority of existing fillers include materials of short duration (i.e., collagen and hyaluronic acid) (Burgess, 2006; Monheit & Coleman, 2006; Narins & Bowman, 2005), which are not suitable for such therapeutic applications. Other permanent (e.g., silicone, polymethylmethacrylate) and semi-permanent (e.g., PLLA and calcium hydroxylapatite) synthetic fillers exist, but none are currently Food and Drug Administration (FDA)-approved for all indications. In addition, while they may improve the quality of life in some patients without adverse effects, the risk of complications may likely outweigh their potential benefit (Colombo, Caregnato, Stifanese, & Ferrando, 2011). In the event of unfavorable sequelae following treatment with synthetic fillers, invasive surgical excision of the injected bulking agent may be attempted but is often unsuccessful (Christensen, Breiting, Janssen, Vuust, & Hodgall, 2005; Eppley & Dadvand, 2006; Goldberg, 2009; Requena et al., 2011). A permanent filler material that approximates the properties of native tissue and that can be selectively degraded has yet to be engineered.

Hydrogels synthesized from naturally-derived carbohydrate polymers are advantageous as they aim to recapitulate the natural extracellular matrix (Peppas, Hilt, Khademhosseini, & Langer, 2006; Slaughter, Khurshid, Fisher, Khademhosseini, & Peppas, 2009). Methylcellulose (MC) is a natural, plant-derived, FDA-approved, and inexpensive carbohydrate polymer. It is a derivative of cellulose that has hydrophobic moieties (i.e., methoxy groups), which afford thermo-gelation properties (Haque & Morris, 1993; Sarkar, 1979) that can be exploited for injectable biomaterial applications. MC also has the appeal of potentially long-term residence in the body, given that humans lack the cellulose-digesting enzyme, cellulase. Moreover, the potential for reversibility exists since cellulase can be selectively administered if the need arises. Polysaccharides, including MC, can be functionalized (Reeves, Ribeiro, Lombardo, Boyer, & Leach, 2010) with methacrylate groups that enable covalent crosslinking of polymer chains via free-radical polymerization. Previously, methacrylated MC has been crosslinked in the presence of photo-initiators and UV light yielding mechanically stable and cytocompatible gels *in vitro*

and *in vivo* (Stalling, Akintoye, & Nicoll, 2009). However, the need for UV light hinders clinical translation due to the limited penetration depth of UV light through human skin (Elisseeff et al., 1999; Gramlich, Holloway, Rai, & Burdick, 2014; Weissleder, 2001).

Alternative polymerization schemes using reduction/oxidation (redox)-initiation systems allow for *in situ* chemical crosslinking, enabling spontaneous gelation at the site of injection under physiological conditions (Van Tomme, Storm, & Hennink, 2008). Ammonium persulfate (APS)/ N,N,N',N'-tetramethylethylenediamine (TEMED) is a redox initiation system employed ubiquitously in crosslinking of hydrogels (Ahmed, 2013; Desai, Tang, Ross, & Gemeinhart, 2012; Fang, Wang, Zhang, Shao, & Chen, 2013; Hennink & van Nostrum, 2002; Hong, Mao, & Wang, 2006; Mironi-Harpaz, Wang, Venkatraman, & Seliktar, 2012; Suhag, Bhatnagar, & Singh, 2008; Yang et al., 2013). However, potential toxicity concerns have been reported (Desai et al., 2012; Hennink & van Nostrum, 2002; Ifkovits et al., 2010; Mironi-Harpaz et al., 2012) as with other photo-initiation systems (Baroli, 2006; Mironi-Harpaz et al., 2012; Page et al., 2013). Therefore, supplanting TEMED with an alternative reducing agent, ascorbic acid (AA), which is a natural metabolite and recognized form of vitamin C, is appealing. Hence, the objective of this study was to engineer injectable, covalently crosslinkable MC hydrogels that can undergo *in situ* gelation using an APS-AA redox initiation system conducive to clinical translation. The biomechanical, swelling and gelation properties of the cellulosic hydrogels were measured, as were the selective reversibility, cytocompatibility, and long-term stability of the materials *in vitro*.

2. Materials and methods

2.1. Macromer synthesis

Methylcellulose with a molecular weight of 14 kDa and a degree of substitution of ~1.5-1.9 for the methoxy groups was purchased from Sigma (St Louis, MO). Methylcellulose was functionalized with methacrylate groups by the esterification of hydroxyl groups to form methacrylated MC (Fig. 1) according to previously published protocols (Burdick, Chung, Jia, Randolph, & Langer, 2005; Gold et al., 2014; Smeds & Grinstaff, 2001; Stalling et al., 2009). Briefly, a solution of 1 wt% 14 kDa MC in RNAse/ DNAse-free water was reacted with

methacrylic anhydride (Sigma) in 20-fold excess (based on a theoretical modification of 10%) for 24 hours at 4°C with periodic adjustments to pH 8.0. The methacrylated MC solution was dialyzed for 72 hours to remove excess, unreacted methacrylic anhydride. The purified MC solution was lyophilized and the final product was stored at -20°C.

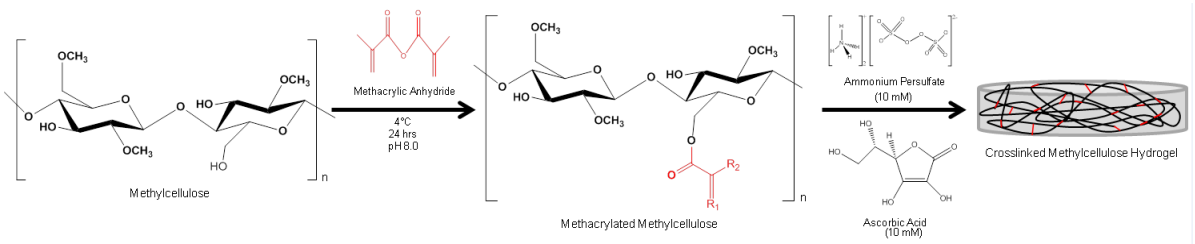

Figure 1: Schematic of methacrylated MC synthesis and hydrogel fabrication using ammonium persulfate and ascorbic acid redox initiators.

The degree of methacrylation was confirmed by ^{1}H-NMR (300 MHz, Varian Mercury 300; Agilent Technologies) following acid hydrolysis of the purified MC as was previously described (Gold et al., 2014; Gupta, Cooper, & Nicoll, 2011). The relative integrations of methacrylate proton peaks (methylene, δ = 6.1 and 5.7 ppm; methyl, δ = 1.9 ppm) to carbohydrate protons was used to determine the molar percentage of methacrylation.

Additional chemical characterization of the MC polymer before and after methacrylation was performed using transmission Fourier transform infrared spectroscopy (FTIR) on samples prepared in KBr pellets. Spectra were acquired using a Nicolet 6700 spectrometer (Thermo Fisher Scientific) at a resolution of 4 cm^{-1} by accumulation of 64 scans in the range of 500 – 4000 cm^{-1}.

2.2. Hydrogel fabrication

Methacrylated MC was dissolved in Dulbecco's Phosphate-Buffered Saline (DPBS) at final macromer concentrations of 2, 3 and 4% (wt/vol) ($MC_{2\%}$, $MC_{3\%}$, and $MC_{4\%}$, respectively). Polymer solutions were combined with APS and AA (10 mM each) (Gold et al., 2014; Shin, Temenoff, & Mikos, 2003; Temenoff, Shin, Conway, Engel, & Mikos, 2003; Varma, Gold, Taub, & Nicoll, 2014) and immediately cast into custom-made glass casting devices with a polysulfone insert. The mixtures were allowed to set for 15 min at room temperature to form cylindrical gels with a thickness of 2 mm and a diameter of 5 mm (unless indicated otherwise).

^{1}H-NMR analysis was performed on acid hydrolyzed $MC_{2\%}$ hydrogels to confirm crosslinking as indicated by the disappearance of characteristic peaks associated with the methacrylate protons (as described above in section 2.1). Transmission FTIR was used to characterize lyophilized $MC_{4\%}$ hydrogels as described above in section 2.1.

2.3. Mechanical testing

Unconfined compression testing was conducted on $MC_{2\%}$, $MC_{3\%}$, and $MC_{4\%}$ hydrogels (n = 4-5) using a custom-built apparatus as previously reported (Chou & Nicoll, 2009; Gold et al., 2014; Gupta et al., 2011; Reza & Nicoll, 2010b). Briefly, the testing protocol consisted of a creep test followed by a multi-ramp stress-relaxation test. The creep test consisted of a 1 g tare load at a ramp velocity of 10 μm s^{-1} for 2700 s until equilibrium was reached (equilibrium criterion: <10 μm displacement in 10 min). The multi-ramp stress relaxation test was conducted using three 5% strain ramps, each followed by a 2000 s relaxation time. Equilibrium Young's modulus (E_y) was determined as the slope of the equilibrium stress (calculated at each ramp) versus applied strain curve. Peak stress (σ_{pk}) was measured at the ramp corresponding to 15% strain.

2.4. Swelling ratio and related physical properties

The equilibrium weight swelling ratio, Q_w, was measured for $MC_{2\%}$, $MC_{3\%}$, and $MC_{4\%}$ constructs 8-mm in diameter (n = 4). Following casting, hydrogels were placed in wells containing DPBS, allowed to swell overnight at 37°C, and then dried by lyophilization. Q_w was calculated as:

$$Q_w = \frac{W_s}{W_d} \quad (1)$$

where W_s and W_d are the weights of the gel in the swollen and dried states, respectively, as described earlier (Gold et al., 2014; Stalling et al., 2009; Varma et al., 2014).

The physical parameters, crosslinking density (v_e) and mesh size (ξ) were calculated based on the Flory-Rehner model as was previously described (Baier Leach, Bivens, Patrick, & Schmidt, 2003; de Jong, van Eerdenbrugh, van Nostrum, Kettenes-van den Bosch, & Hennink, 2001; Flory, 1953; Metters, Anseth, & Bowman, 1999). Briefly, the volumetric swelling ratio

(Q_v) was determined from the mass swelling ratio, Q_w (Baier Leach et al., 2003; Marsano, Gagliardi, Ghioni, & Bianchi, 2000) according to:

$$Q_v = 1 + \left(\frac{\rho_p}{\rho_s}(Q_w - 1)\right) \quad (2)$$

where ρ_p is the density of the dry polymer (0.276 g/cm^3) (Parsons, 2006) and ρ_s is the density of the solvent (water = 1 g/cm^3). The average molecular weight between crosslinks ($\bar{M}_c$) was calculated using a simplified version of the Flory-Rehner equation (Baier Leach et al., 2003; Metters et al., 1999):

$$Q_v^{5/3} \cong \frac{\bar{v}\bar{M}_c}{V_1}\left(\frac{1}{2} - \chi\right) \quad (3)$$

where $\bar{v}$ is the specific volume of the dry polymer, V_1 is the molar volume of the solvent (water = 18 mol/cm^3), and χ is the Flory polymer-solvent interaction parameter. The value for χ (0.473) was based on the assumption that χ for MC is comparable to that of other polysaccharides (i.e., HA and dextran) due to similar chemical structures (Baier Leach et al., 2003; de Jong et al., 2001; Marsano et al., 2000).

The effective crosslinking density, v_e, was then calculated as (Baier Leach et al., 2003; Huglin, Rehab, & Zakaria, 1986):

$$v_e = \frac{\rho_p}{\bar{M}_c} \quad (4)$$

The swollen hydrogel mesh size, ξ, was determined from the following equation (Baier Leach et al., 2003; de Jong et al., 2001):

$$\xi = Q_v^{1/3}\sqrt{\bar{r}_o^2} \quad (5)$$

where $\sqrt{\bar{r}_o^2}$ is the root-mean square distance between crosslinks. The root-mean-square end-to-end distance value for CMC previously reported as (Cleland, 1970):

$$\sqrt{\frac{\bar{r}_o^2}{2n}} \cong 2.1 \quad (6)$$

was used here (*n* is the degree of polymerization), due to the basic similarity between the backbone of methylcellulose and carboxymethylcellulose. Given that $\sqrt{\bar{r}_o^2}$ is a function of the molecular weight, the following relationship was derived:

$$\sqrt{\bar{r}_o^2} = 0.217\sqrt{M_n} \quad (7)$$

for MC, with n = 75 at a molecular weight (M_n) of 14 kDa (Baier Leach et al., 2003). Based on equations 5 and 7 and the substitution of $\bar{M}_c$ for M_n, the mesh size was calculated using the equation (Baier Leach et al., 2003):

$$\xi = 0.217\sqrt{\bar{M}_c}Q_v^{1/3} \quad (8)$$

The values determined for v_e and ξ are considered approximations given the assumptions made in the Flory-Rehner calculations.

2.5. Rheometry

Rheological analysis was conducted on $MC_{2\%}$ and $MC_{4\%}$, representing the extremes of the range of macromer concentrations investigated. Experiments were performed at room temperature (n = 4-7) using an AR2000ex Rheometer (TA Instruments, New Castle, DE) equipped with a cone and plate geometry (2°, 40 mm). Preliminary strain and frequency sweep measurements on non-gelled methacrylated MC polymer solutions established the optimal test parameters (0.5% strain, 1Hz) based on the linear viscoelastic region (Tadros, 2010). Time zero was considered as the point at which the initiators were mixed. Gelation onset, determined by oscillation measurement (time sweep), was defined at G'/G'' = 1, corresponding to the crossover point of G' and G'', where G' and G'' are the elastic and viscous moduli, respectively (Winter & Chambon, 1986). Gelation completion was identified as the first time at which four consecutive values of the growth of G' exhibited less than a 2% change (Gold et al., 2014; Temenoff et al., 2003). The phase angle, δ, describing the relative viscous and elastic behavior (S. Falcone & Berg, 2009; Su, Chen, & Lin, 2010), as well as the complex viscosity, $|\eta^*|$, were also measured. The results were analyzed using the TA Data Analysis software (Advantage v5.4.0).

2.6. Cellulase degradation

To test the reversibility of $MC_{2\%}$ and $MC_{4\%}$ hydrogels using cellulase enzymatic treatment, gels were immersed in cellulase solution and degradation was monitored over time. Hydrogels (8 mm diameter) were cast and incubated in DPBS to equilibrate overnight at 37°C, after which initial wet weight was measured. The gels were then placed in 100 U/mL cellulase solution derived from *Trichoderma viride* at 37°C for varying amounts of time over 24 hours. At each time point, the gels (n = 4) were blotted with filter paper to remove excess liquid (Gold et al., 2014; Reeves et al., 2010), and gross images were captured using a stereomicroscope (Stemi 2000-C) with Zeiss AxioVision software (Thornwood, NY) to visualize qualitative structural changes. Wet weights were recorded to track weight loss over time and to calculate the degradation rate.

2.7. Cytocompatibility

Cytocompatibility of MC hydrogels was evaluated by co-culturing neonatal human dermal fibroblasts in the presence of $MC_{2\%}$ and $MC_{4\%}$ gels. Fibroblasts were plated at 15,000 cells per well in tissue culture-treated polystyrene 24-well plates with DMEM high glucose media supplemented with 10% fetal bovine serum (Invitrogen), 100 U/mL penicillin, and 100 µg/mL streptomycin. On day 0, transwell inserts (polyethylene terephthalate membranes with a 3.0 µm pore size) were placed in each well along with a hydrogel disk; hydrogel-free cell monolayers served as controls. Cell viability was assessed using the Live/Dead kit (Invitrogen) for visualization (n = 2) and DNA content was quantified with the Quant-iT™ PicoGreen assay kit (Invitrogen/Molecular Probes) as a measure of proliferation (n = 4) on days 1 and 4. Samples were rinsed in serum-free medium and incubated in Live/Dead solution (0.75 mM calcein AM, 0.75 mM ethidium homodimer-1) for 30 min. Images were captured using a Zeiss Axio Observer microscope with fluorescent capabilities at excitation/emission wavelengths of 494/517 nm and 528/617 nm for calcein AM and ethidium homodimer-1, respectively. For DNA quantification, medium was aspirated and the cells were rinsed with DPBS, replaced with 0.5 mL lysis buffer (10 mM Tris(hydroxymethyl)aminomethane, 0.1% (v/v) Triton X-100) and kept on ice for 15 minutes. The wells were then scraped and the solution collected to be tested with the Quant-iT™ PicoGreen assay kit, as per manufacturer's instructions. Calf thymus DNA standards were used for determining the concentration of DNA.

2.8. Mechanical stability

To quantify the potential effect of hydrolysis on long-term stability, $MC_{2\%}$ and $MC_{4\%}$ hydrogels were maintained at 37°C in DPBS buffer over 12 weeks, during which mechanical properties were assessed. The buffer was replaced three times per week, and following intervals of two-weeks, gels underwent unconfined compression testing, to determine E_y as described earlier. In addition, stereomicrographs of the gels were captured at each time point for visual assessment.

2.9. Statistical analysis

A 1-way ANOVA with a Tukey's post-hoc test was used to determine the effect of macromer concentration on the material properties (Q_w, v_e, ξ, E_y, σ_p), and rheological properties (gelation times, G', G'', δ, $|\eta^*|$), as well as the effect of time on E_y of $MC_{4\%}$ hydrogels. A 2-way ANOVA with a Tukey's post-hoc test was used to determine the effect of time and hydrogel co-culture on DNA content. Significance was set at $p < 0.05$. All data represent the mean ± standard deviation. Statistical analyses were performed using JMP software (SAS Institute, Cary, NC).

3. Results

3.1. Spectroscopic Analyses

^{1}H-NMR confirmed the percent methacryation along the MC polymer backbone to be 3.3% with a degree of methacrylate substitution (DS) of 0.1 (based on a maximum DS of 3) (Fig. 2A). In addition, the disappearance of the peaks attributed to the methylene and methyl protons of the methacrylate group indicates formation of the interchain single carbon bond crosslinks in the hydrogel upon redox polymerization (Fig. 2B). Transmission FTIR also corroborated the composition of the modified MC polymer and crosslinked hydrogel (Fig. 3). The carbonyl (C=O) of the methacrylate group is present in the spectra for both the methacrylated MC and the $MC_{4\%}$ hydrogel at ~1710 cm^{-1}. The alkene (C=C) of the methacrylate is indicated by an asymmetrical peak at ~1640 cm^{-1}, which overlaps with an existing smooth peak in MC also at ~1640 cm^{-1}. The peak at 1100 cm^{-1} is indicative of C-O-C stretching and the peak at 3410 cm^{-1} corresponds to hydroxyl groups present on the MC backbone.

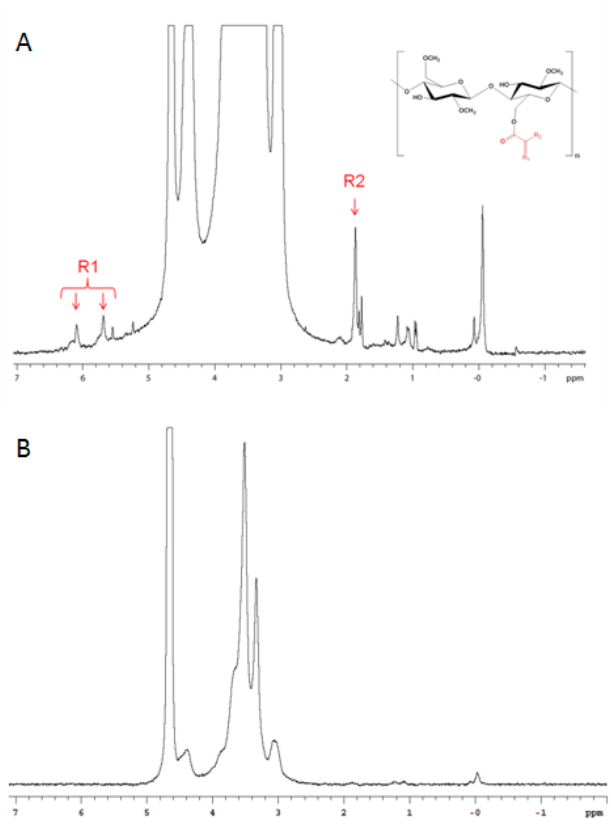

Figure 2: Representative ^{1}H-NMR spectra of (A) modified MC indicating peaks associated with the methacrylate groups on the MC polymer backbone, and of (B) a crosslinked MC hydrogel. R1 represents the methylene protons and R2 corresponds to the methyl protons of the methacrylate group.

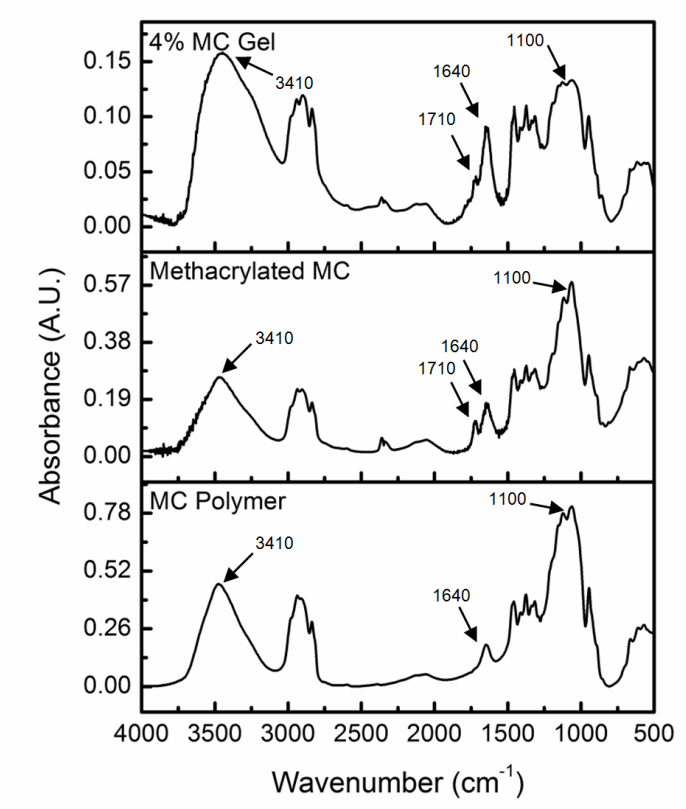

Figure 3: Representative transmission FTIR spectra of the MC base polymer, methacrylated MC polymer, and the lyophilized $MC_{4\%}$ hydrogel. Black arrows indicate characteristic peaks of MC and methacrylate groups referenced in the text.

3.2. Mechanical properties

The compressive mechanical properties of $MC_{2\%}$, $MC_{3\%}$ and $MC_{4\%}$ hydrogels were obtained via unconfined compression testing. E_y and σ_{pk} significantly increased as a function of increasing macromer concentration. By varying the MC macromer concentration between 2% (w/v) and 4% (w/v), E_y ranged from 1.47 ± 0.33 to 5.31 ± 0.71 kPa, and σ_{pk} ranged from 0.45 ± 0.09 to 1.06 ± 0.15 kPa, with $MC_{4\%}$ hydrogels maintaining the highest values for both properties, which were significantly different relative to all other groups (Fig. 4A-B).

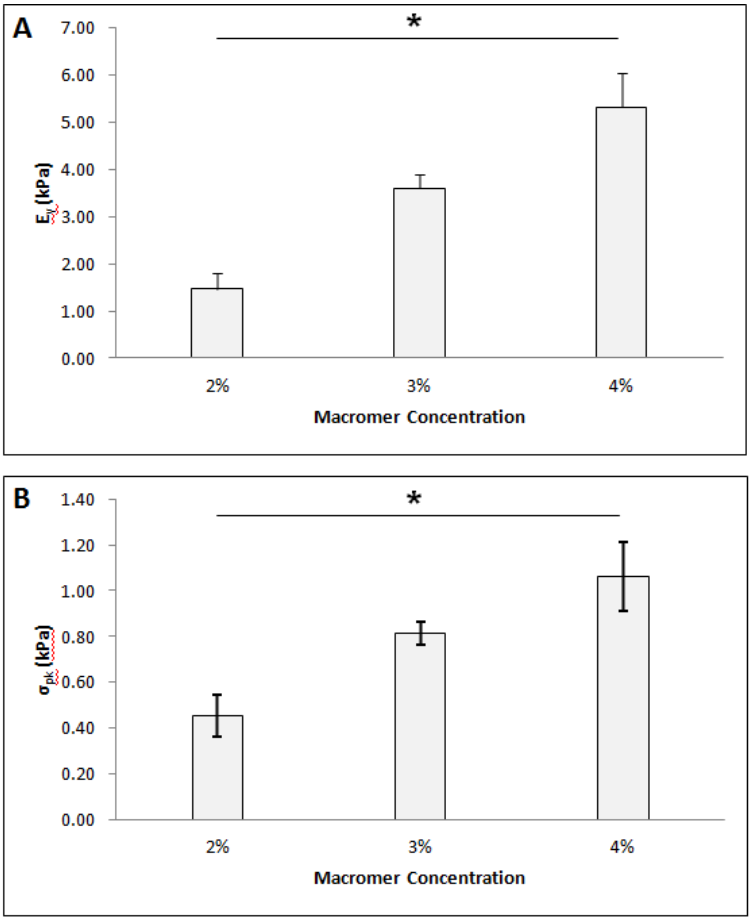

Figure 4: Equilibrium mechanical properties of MC hydrogels as a function of macromer concentration. (A) Equilibrium Young's modulus, E_y and (B) peak stress, σ_{pk}. Significance set at $p < 0.05$: *, significantly different with respect to all other groups.

3.3. Swelling and related physical properties

For each macromer concentration group ($MC_{2\%}$, $MC_{3\%}$ and $MC_{4\%}$), the physical properties investigated (Q_w, v_e, ξ) were all significantly different from each other. The range of Q_w was from 33.19 ± 0.79 to 56.10 ± 1.94, with increasing values associated with decreasing macromer concentration (Table 1). Similarly, the $MC_{4\%}$ gels exhibited the lowest ξ values, (42.86 ± 1.11 nm) and the $MC_{2\%}$ samples the highest (76.38 ± 2.94 nm), while v_e spanned from $3.27 \times 10^{-5} \pm 1.21 \times 10^{-6}$ mol/cm^3 for the $MC_{4\%}$ gels to $1.43 \times 10^{-5} \pm 8.24 \times 10^{-7}$ mol/cm^3 for the $MC_{2\%}$ group (Table 1).

Table 1: Swelling ratio and related physical properties of MC hydrogels. Equilibrium weight swelling ratio, Qw; effective crosslinking density, v_e; and hydrogel mesh size, ξ. Significance set at $p < 0.05$: [a] significantly different with respect to all other groups.

Macromer concentration	Q_w	v_e (mol/cm^3)	ξ (nm)
2%	56.10 ± 1.94 [a]	1.43E-05 ± 8.24E-07 [a]	76.38 ± 2.94 [a]
3%	38.55 ± 2.35 [a]	2.61E-05 ± 2.59E-06 [a]	50.45 ± 3.36 [a]
4%	33.19 ± 0.79 [a]	3.27E-05 ± 1.21E-06 [a]	42.86 ± 1.11 [a]

297

298 *3.4. Gelation properties*

299 Gelation properties were evaluated for $MC_{2\%}$ and $MC_{4\%}$ using rheological testing.
300 Gelation onset occurred within ~2 min, irrespective of macromer concentration, but gelation
301 completion for $MC_{2\%}$ gels (21.03 ± 1.70 min) was significantly different from that of $MC_{4\%}$
302 samples (15.02 ± 0.54 min; Fig. 5, Table 2). δ precipitously decreased at gelation onset, and
303 approached zero (~0.64 ± 0.22 average for both groups) at gelation completion, while $|\eta^*|$ was
304 low initially but significantly increased with gelation completion for both MC formulations. The
305 value of G' at gelation completion was 937.9 ± 323 Pa for $MC_{4\%}$ hydrogels, significantly
306 different from the $MC_{2\%}$ group (245.3 ± 52.7 Pa; Table 2).

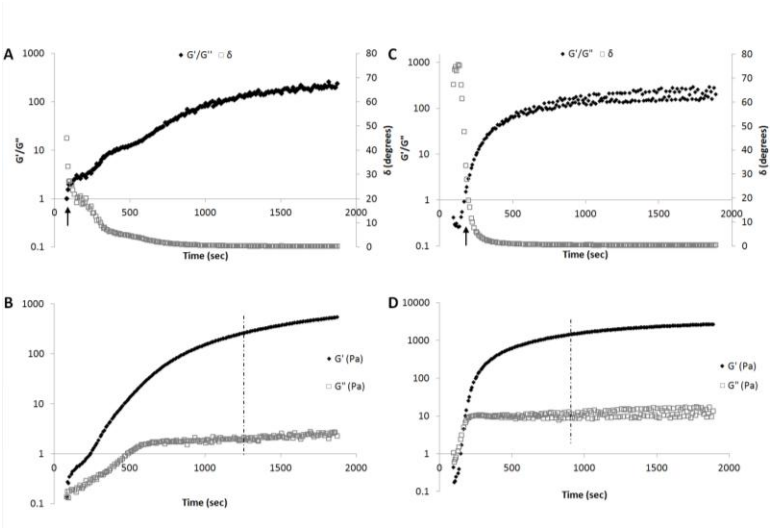

307

308 **Figure 5:** Representative graphs of the evolution of rheological properties during the redox-polymerization of $MC_{2\%}$
309 (A, B) and $MC_{4\%}$ (C, D). (A, C) Gelation onset, defined as *G'/G"*=1, is indicated by the arrow. The phase shift, δ
310 (right axis), is also shown. (B,D) Gelation completion, defined as the first time at which there were at least four
311 consecutive points with less than 2% change in *G'*, is indicated by the vertical line. The concurrent evolution of *G"*
312 is also graphed, and the x-axes of the vertical panels are aligned to allow for direct comparison between curves.

Table 2: Gelation/rheological properties of redox-polymerized $MC_{2\%}$ and $MC_{4\%}$ hydrogels. Storage modulus, G'; Loss modulus, G"; the phase angle, δ; complex viscosity, $|\eta^*|$. Significance set at $p < 0.05$: [a], significantly different from other gelation time within macromer concentration; [b], significantly different from other macromer concentration within gelation time

	Macromer Concentration (w/v)	Time (min)	*G'* (Pa)	*G''* (Pa)	δ	$\lvert\eta^*\rvert$ (Pa·s)
Gelation Onset	2%	1.58 ± 0.67 [a]	1.93 ± 1.87 [a]	0.80 ± 0.68 [b]	28.28 ± 13.52 [a,b]	0.35 ± 0.30 [a]
	4%	2.25 ± 1.02 [a]	2.73 ± 1.92 [a]	2.50 ± 2.16 [a,b]	39.04 ± 7.65 [b]	0.59 ± 0.46 [a]
Gelation Completion	2%	21.03 ± 1.70 [a,b]	245.3 ± 52.72 [a,b]	2.70 ± 0.98 [b]	0.66 ± 0.26 [a,b]	39.11 ± 8.43 [a,b]
	4%	15.02 ± 0.54 [a,b]	937.9 ± 322.8 [a,b]	9.29 ± 1.04 [a,b]	0.61 ± 0.17	149.2 ± 51.3 [a,b]

3.5. Enzymatic degradation

Enzymatic treatment of $MC_{2\%}$ and $MC_{4\%}$ hydrogels with cellulase resulted in complete degradation within 24 hours. Exposure to the enzyme initially caused the gels to swell (Fig. 6A-C). With increased exposure, gel borders became less defined, and the constructs became progressively more amorphous, until they completely disintegrated (Fig. 6). $MC_{2\%}$ hydrogels degraded rapidly, exhibiting no structure by 2 hours. The degradation profile of the $MC_{4\%}$ hydrogels was corroborated by progressive weight loss measurements over the 24-hour duration (Fig. 6D). The degradation rate was 3.9 mg/hr between 4-16 hours and increased to 10.4 mg/hr between 16-24 hours.

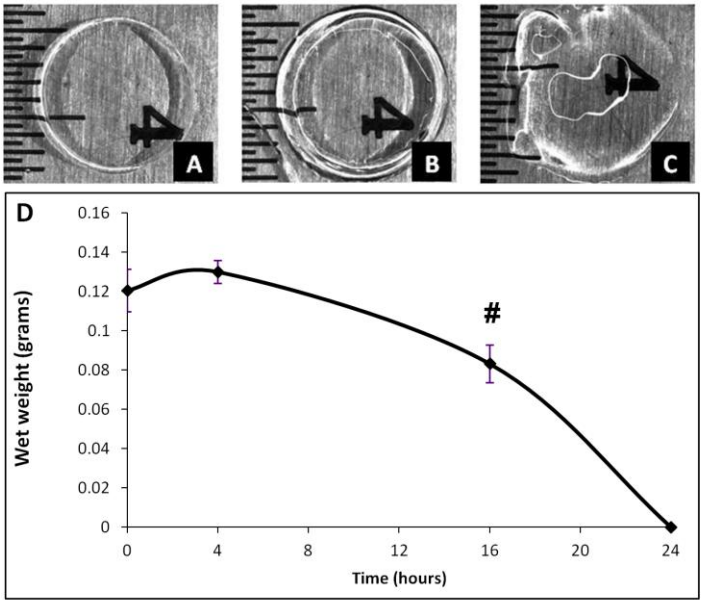

Figure 6: Enzymatic degradation assessment. Representative stereomicrographs of $MC_{4\%}$ constructs (A) 0, (B) 4, and (C) 16 hours after cellulase treatment. Complete degradation was observed by 24 hours. Scale is in mm. (D) Wet weight of $MC_{4\%}$ hydrogels as a function of exposure time to cellulase. Significance set at $p < 0.05$: #, significant relative to 0 and 4 hours.

3.6. Cytocompatibility

Following four days in co-culture with $MC_{2\%}$ and $MC_{4\%}$ hydrogels, human dermal fibroblasts were viable and displayed an elongated fibroblastic morphology, comparable to hydrogel-free controls (Fig. 7A-C). In addition, there was no statistical difference between the DNA content of cells in co-culture with the $MC_{2\%}$ and $MC_{4\%}$ hydrogels and hydrogel-free controls (Fig. 7D).

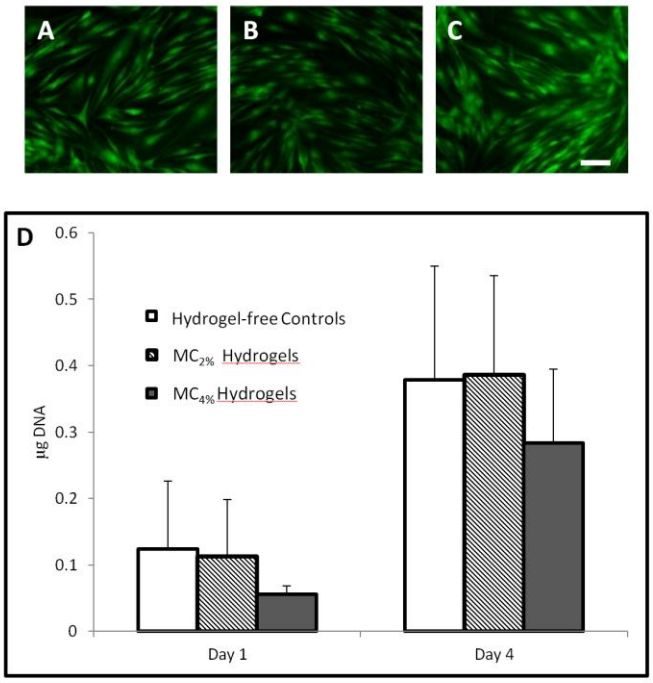

Figure 7: Cell viability analysis. Representative Live/Dead fluorescent images of fibroblasts following 4 days of co-culture (A) without (control), (B) with $MC_{2\%}$, and (C) with $MC_{4\%}$ hydrogels. Live cells are stained green (with calcein AM) and dead cells are shown in red (with ethidium homodimer). Scale bar = 50 μm. (D) DNA content of fibroblasts co-cultured with $MC_{2\%}$ and $MC_{4\%}$ hydrogels. Significance set at $p < 0.05$: No statistical difference relative to the control of the corresponding day.

3.7. Mechanical stability

The $MC_{4\%}$ gels largely maintained their functional structure and shape over time, as the E_y at 12 weeks (3.029 ± 0.68 kPa) was not significantly different from that at 2 weeks (4.09 ±0.78 kPa) (Fig. 8). However, the $MC_{2\%}$ gels were too weak to undergo mechanical testing even at two weeks.

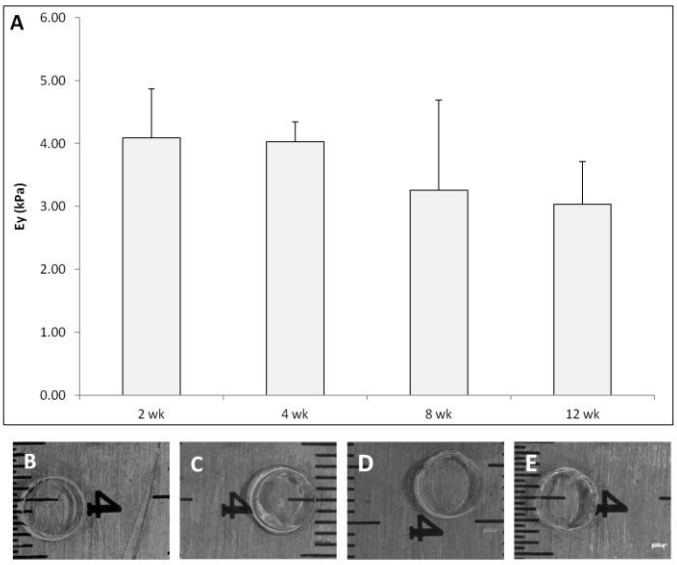

Figure 8: Mechanical Stability. (A) The E_y values of $MC_{4\%}$ constructs measured over 12 weeks. Significance set at $p < 0.05$: there was no statistical difference among the time points. Stereomicrographs of representative gels at (B) 1, (C) 4, (D) 8, and (E) 12 weeks after initial casting. Scale is in mm.

4. Discussion

There is a significant demand for injectable, long-term, biocompatible soft tissue filler materials. The present study was motivated by prior work describing the fabrication of biocompatible MC hydrogels using photopolymerization (Stalling et al., 2009), a method which inherently limits clinical translation. An alternative minimally invasive and cytocompatible technique, specifically the APS-AA redox polymerization system, was employed here to produce covalently crosslinked MC hydrogels. This may be a promising approach for engineering injectable gels that are biocompatible and mechanically stable. Moreover, the versatility of the system allows for tuning the properties for an array of soft tissue augmentation applications.

Matching properties of hydrogels to native tissue is desired for stability and functionality. The mechanical and physical (i.e., swelling) properties of the MC gels demonstrate their utility as tissue fillers. The gels exhibited E_y values that ranged from 1.47 ± 0.33 - 5.31 ± 0.71 kPa, comparable to human adipose tissue, with moduli reported to be 3.25 ± 0.91 kPa (Samani, Zubovits, & Plewes, 2007). In addition, the swelling ratios are indicative of efficient water retention (Coviello, Matricardi, Marianecci, & Alhaique, 2007; Liu, Liu, Wang, Guocheng, & Chen, 2007), approximating the hydrated soft tissue of interest. The functional material properties including equilibrium compressive modulus, peak stress, and crosslinking density

were improved with increasing macromer concentration, in line with previous findings (Burdick et al., 2005; Chou & Nicoll, 2009; Gold et al., 2014; Kablik, Monheit, Yu, Chang, & Gershkovich, 2009; Stalling et al., 2009). In accordance with the theory of rubber elasticity, as macromer concentration increases, hydrogel stiffness increases with a concomitant decrease in swelling ratio and mesh size (Anseth, Bowman, & Brannon-Peppas, 1996; Canal & Peppast, 1989; Gold et al., 2014; Krouskop, Wheeler, Kallel, Garra, & Hall, 1998; Levental, Georges, & Janmey, 2007; Oudshoorn, Rissmann, Bouwstra, & Hennink, 2006; Reza & Nicoll, 2010a; Stalling et al., 2009). Consistent with this theory, and with previous work, $MC_{4\%}$ gels exhibited the highest crosslinking density, and lowest swelling ratio and mesh size. Still, the effect and optimization of additional fabrication parameters, such as MC molecular weight and methacrylation percentage, will require further investigation. Although these parameters impact hydrogel bulk properties, they can also influence solution viscosities and mixing efficiency, and thus affect sample preparation (Gold et al., 2014; Varma et al., 2014), injectability and eventual adoption in the clinic.

Rheological measurements were used to characterize functional properties related to injection, and demonstrated the advantages of MC as an *in situ* gelation system with regard to ease of handling and administration. In practice, translation of this system to the clinic will be implemented by loading MC/APS and MC/AA in separate barrels of a dual-barrel syringe equipped with a mixing tip, in which the crosslinking reaction will be initiated (Ifkovits et al., 2010; Milani, Freemont, Hoyland, Adlam, & Saunders, 2012). Low initial viscosity ($|\eta^*|$) predicts ease of delivery using a fine-gauge needle (Ho, Lowman, & Marcolongo, 2006); while high viscosity (afforded by both the intrinsic thermogelation property of MC and the radical crosslinking) can prevent extravasation of material away from the injection site ((Page et al., 2013). The $|\eta^*|$ values for uncrosslinked, pre-polymerized MC were ~ 1 Pa·s (Table 2) and those post-gelation for $MC_{4\%}$ were orders of magnitude greater (149.2 ±51.3 Pa·s), and on par with Juvederm Ultra, a commercial injectable HA filler, which exhibits the same properties pre- and post-injection (197.53 ±26.25 Pa·s based on Varma et al., 2014, and ~152 Pa·s reported by S. J. Falcone & Berg, 2008). Values of δ post-gelation were two orders of magnitude less than those at gelation onset, consistent with the progression towards completely elastic behavior associated with gelation. Gelation properties are indicative of the time-frame for manipulation by surgeons,

and gelation onset and completion values were measured to be within the ISO Standard 5833/1–1999 E for injectable materials (4-15 min).

Cytocompatibility of redox-polymerized MC gels was confirmed by the DNA content as well as the phenotypic fibroblastic morphology of the cells in co-culture with the hydrogels, irrespective of MC macromer concentration. As with other chemical crosslinking systems, ascorbic acid may exhibit a concentration-dependent toxicity. However, when $MC_{2\%}$ and $MC_{4\%}$ hydrogels produced with 10 mM ascorbic acid were placed in co-culture with cells, they elicited the same response as the hydrogel-free controls, thus ruling out potential toxicity due to residual free radicals and ascorbic acid. This may be due to the low concentration (10 mM) of ascorbic acid used, in comparison to other studies (100 mM) (Shin et al., 2003).

While it is intended that fillers last long term and do not undergo degradation, the selective reversibility is an attractive feature, offering ease of correction in the event of complications or malposition. Adverse sequelae of synthetic permanent fillers may not be safely remedied, as corrective measures and management often involve steroid treatments or surgical excision, which are invasive, often unsuccessful, and negate the original attempt at correction (Christensen et al., 2005; Eppley & Dadvand, 2006; Goldberg, 2009; Requena et al., 2011). Natural-based fillers, in contrast, can conveniently be selectively reversed via a degradative enzymatic treatment. Comparable to the current clinical practice of administering hyaluronidase to degrade HA-based fillers (Hirsch, Brody, & Carruthers, 2007; Rzany, Becker-Wegerich, Bachmann, Erdmann, & Wollina, 2009), digestion of the proposed MC-based fillers would be possible using cellulase. Furthermore, cellulase may offer an advantage over hyaluronidase in that it is exclusive for cellulosic polysaccharides, which are not endogenous to humans, whereas hyaluronidase may target HA in neighboring connective tissue, with potential deleterious repercussions. Complete degradation of the MC constructs with cellulase at 100 U/mL occurred within 24 hours, which is on par with the clinical reports of enzymatic degradation of HA-based fillers with hyaluronidase (75–150 U/mL) by 72 hours (Hirsch et al., 2007; Rzany et al., 2009). Initially, the gels began to swell upon exposure to cellulase, as chain scission allowed for increased water uptake and an overall gain in wet weight. However, with increasing exposure to the enzyme and greater access to the polysaccharide backbone, the degradation rate increased and substantial mass loss was observed. Still, additional *in vivo* testing will be necessary to

assess both the efficiency of cellulase in digesting MC hydrogels in the body as well as the potential inflammatory response that may be elicited from the enzyme itself. Although concern over immunogenicity is warranted, cellulase derived from *Trichoderm*a has been shown to be cytocompatible with rat cardiac cells (Entcheva et al., 2004) and human fibrosarcoma cells (Al-Abboodi et al., 2014), as well as biocompatible *in vivo* when injected subcutaneously in Lewis rats (Al-Abboodi, Fu, Doran, Tan, & Chan, 2013).

The stability of the constructs in aqueous environments is directly impacted by fabrication parameters; the gels of low macromer concentration (i.e., $MC_{2\%}$) were susceptible to hydrolytic degradation, and the E_y could not be measured after 2 weeks, while the values of the $MC_{4\%}$ hydrogels did not display a statistically significant decrease between 2 and 12 weeks. These results are corroborated by a prior study involving subcutaneous implantation of photopolymerized MC hydrogels in CD-1 mice, whereby 6% (w/v) MC gels (in contrast to 2% (w/v) MC gels) maintained their original dimensions and structural integrity for 80 days *in vivo*. This was supported by E_y values that were not significantly different prior to or post implantation (Stalling et al., 2009). However, qualitative visual assessment of APS-AA crosslinked gels ($MC_{4\%}$) suggested a decrease in gel size with time. Since the long-term stability of these hydrogels is a key factor for their intended application and presents a potential competitive advantage, the versatility of the MC platform should be exploited to engineer more stable gels that are long-lasting. Specifically, increasing the methacrylation percentage and/or molecular weight of the initial polymer, may improve the longevity of these constructs.

5. Conclusions

Methacrylated MC macromers were covalently crosslinked using the APS-AA redox-initiation system to form cytocompatible hydrogels that represent a novel platform for injectable soft tissue fillers. Cellulosic hydrogels fabricated using the ascorbic acid-based, redox-initiation system have the appeal of natural, cost-effective and biologically-friendly components. Furthermore, the possibility of selective reversibility is a compelling feature from a clinical standpoint, and provides a distinct benefit over alternative synthetic fillers. Finally, the ease of handling and administration, and the ability to tune the mechanical and physical properties, underscore the versatility of this *in situ* gelling MC system for a range of applications in plastic and reconstructive surgery.

Acknowledgements

This work was supported in part by a grant from the National Science Foundation (DMR 1207480) and by a sponsored research agreement with the Procter & Gamble Co. The authors wish to thank Dr. Padmanava Pradhan for technical assistance with ^{1}H-NMR spectroscopy, as well as Dr. Adele L. Boskey and Dr. Patrick E. Donnelly (Hospital for Special Surgery, New York, NY) for valuable assistance with FTIR spectroscopy.

References

Ahmed, E. M. (2013). Hydrogel: Preparation, characterization, and applications. *Journal of Advanced Research*. doi:10.1016/j.jare.2013.07.006

Al-Abboodi, A., Fu, J., Doran, P. M., Tan, T. T. Y., & Chan, P. P. Y. (2013). Injectable 3D hydrogel scaffold with tailorable porosity post-implantation. *Advanced Healthcare Materials*, *3*, 725–736. doi:10.1002/adhm.201300303

Al-Abboodi, A., Tjeung, R., Doran, P. M., Yeo, L. Y., Friend, J., & Yik Chan, P. P. (2014). In situ generation of tunable porosity gradients in hydrogel-based scaffolds for microfluidic cell culture. *Advanced Healthcare Materials*, 1655–1670. doi:10.1002/adhm.201400072

Anseth, K., Bowman, C., & Brannon-Peppas, L. (1996). Mechanical properties of hydrogels and their experimental determination. *Biomaterials*, *17*(17), 1647–1657.

Baier Leach, J., Bivens, K. A., Patrick, C. W., & Schmidt, C. E. (2003). Photocrosslinked hyaluronic acid hydrogels: natural, biodegradable tissue engineering scaffolds. *Biotechnology and Bioengineering*, *82*(5), 578–89. doi:10.1002/bit.10605

Baroli, B. (2006). Photopolymerization of biomaterials: issues and potentialities in drug delivery, tissue engineering, and cell encapsulation applications. *Journal of Chemical Technology & Biotechnology*, *81*(4), 491–499. doi:10.1002/jctb.1468

Barton, S. E., Engelhard, P., & Conant, M. (2006). Poly-L-lactic acid for treating HIV-associated facial lipoatrophy: a review of the clinical studies. *International Journal of STD & AIDS*, *17*(7), 429–435. doi:10.1258/095646206777689116

Burdick, J., Chung, C., Jia, X., Randolph, M., & Langer, R. (2005). Controlled degradation and mechanical behavior of photopolymerized hyaluronic acid networks. *Biomacromolecules*, *6*(1), 386–391.

Burgess, C. (2006). Principles of soft tissue augmentation for the aging face. *Clinical Interventions in Aging*, *1*(4), 349–355.

Canal, T., & Peppast, N. A. (1989). Correlation between mesh size and equilibrium, *23*, 1183–1193.

Chou, A. I., & Nicoll, S. B. (2009). Characterization of photocrosslinked alginate hydrogels for nucleus pulposus cell encapsulation. *Journal of Biomedical Materials Research Part A*, *91A*(1), 187–194. doi:10.1002/jbm.a.32191

Christensen, L., Breiting, V., Janssen, M., Vuust, J., & Hodgall, E. (2005). Adverse Reactions to Injectable Soft Tissue Permanent Fillers. *Aesthetic Plastic Surgery*, *29*, 34–48.

Cleland, R. L. (1970). Ionic polysaccharides. IV. Free-rotation dimensions for disaccharide polymers. Comparison with experiment for hyaluronic acid. *Biopolymers*, *9*(7), 811–824.

Colombo, G., Caregnato, P., Stifanese, R., & Ferrando, G. (2011). Destructive granulomatous reaction to polyacrylamide lip injection: solution for a complex case. *Aesthetic Plastic Surgery*, *35*(4), 662–5. doi:10.1007/s00266-011-9660-9

Coviello, T., Matricardi, P., Marianecci, C., & Alhaique, F. (2007). Polysaccharide hydrogels for modified release formulations. *Journal of Controlled Release : Official Journal of the Controlled Release Society*, *119*(1), 5–24. doi:10.1016/j.jconrel.2007.01.004

De Jong, S. J., van Eerdenbrugh, B., van Nostrum, C. F., Kettenes-van den Bosch, J. J., & Hennink, W. E. (2001). Physically crosslinked dextran hydrogels by stereocomplex formation of lactic acid oligomers: degradation and protein release behavior. *Journal of Controlled Release : Official Journal of the Controlled Release Society*, *71*(3), 261–75.

Desai, E. S., Tang, M. Y., Ross, A. E., & Gemeinhart, R. a. (2012). Critical factors affecting cell encapsulation in superporous hydrogels. *Biomedical Materials (Bristol, England)*, *7*(2), 024108. doi:10.1088/1748-6041/7/2/024108

Drury, J., & Mooney, D. J. (2003). Hydrogels for tissue engineering: scaffold design variables and applications. *Biomaterials*, *24*(24), 4337–4351.

Elisseeff, J., Anseth, K., Sims, D., McIntosh, W., Randolph, M., & Langer, R. (1999). Transdermal photopolymerization for minimally invasive implantation. *Proceedings of the National Academy of Sciences*, *96*(March), 3104–3107. Retrieved from http://www.pnas.org/content/96/6/3104.short

Entcheva, E., Bien, H., Yin, L., Chung, C. Y., Farrell, M., & Kostov, Y. (2004). Functional cardiac cell constructs on cellulose-based scaffolding. *Biomaterials*, *25*, 5753–5762. doi:10.1016/j.biomaterials.2004.01.024

Eppley, B., & Dadvand, B. (2006). Injectable Soft-Tissue Fillers: Clinical Overview. *Plastic and Reconstructive Surgery*, *118*(4), 98e–106e.

Falcone, S., & Berg, R. (2009). Temporary Polysaccharide Dermal Fillers: A Model for Persistence Based on Physical Properties. *Dermatologic Surgery*, *35*(8), 1238–1243.

Falcone, S. J., & Berg, R. a. (2008). Crosslinked hyaluronic acid dermal fillers: a comparison of rheological properties. *Journal of Biomedical Materials Research. Part A*, *87*(1), 264–71. doi:10.1002/jbm.a.31675

Fang, Y., Wang, C.-F., Zhang, Z.-H., Shao, H., & Chen, S. (2013). Robust self-healing hydrogels assisted by cross-linked nanofiber networks. *Scientific Reports*, *3*, 2811. doi:10.1038/srep02811

Flory, P. J. (1953). *Principles of Polymer Chemistry*. Ithaca: Cornell University Press.

Gold, G. T., Varma, D. M., Harbottle, D., Gupta, M. S., Stalling, S. S., Taub, P. J., & Nicoll, S. B. (2014). Injectable Redox-Polymerized Methylcellulose Hydrogels as Potential Soft tissue Filler Materials. *Journal of Biomedical Materials Research. Part A*, *102*, 4536–4544. doi:10.1002/jbm.a.35132

Goldberg, D. J. (2009). Breakthroughs in US dermal fillers for facial soft-tissue augmentation. *Journal of Cosmetic and Laser Therapy : Official Publication of the European Society for Laser Dermatology*, *11*(4), 240–7. doi:10.3109/14764170903341731

Gramlich, W. M., Holloway, J. L., Rai, R., & Burdick, J. a. (2014). Transdermal gelation of methacrylated macromers with near-infrared light and gold nanorods. *Nanotechnology*, *25*(1), 014004. doi:10.1088/0957-4484/25/1/014004

Gupta, M. S., Cooper, E. S., & Nicoll, S. B. (2011). Transforming Growth Factor-Beta 3 Stimulates Cartilage Matrix Elaboration by Human Marrow-Derived Stromal Cells Encapsulated in Photocrosslinked Carboxymethylcellulose Hydrogels: Potential for Nucleus Pulposus Replacement. *Tissue Engineering Part A*, *17*(23-24), 2903–2910.

Haque, A., & Morris, E. R. (1993). Thermogelation of methylcellulose . Part I : molecular structures and processes. *Carbohydrate Polymers*, *22*, 161–173.

Hennink, W. E., & van Nostrum, C. F. (2002). Novel crosslinking methods to design hydrogels. *Advanced Drug Delivery Reviews*, *54*(1), 13–36. Retrieved from http://www.ncbi.nlm.nih.gov/pubmed/11755704

Hirsch, R., Brody, H., & Carruthers, J. (2007). Hyaluronidase in the office: A necessity for every dermasurgeon that injects hyaluronic acid. *Journal of Cosmetic and Laser Therapy*, *9*(3), 182–185.

Ho, E., Lowman, A., & Marcolongo, M. (2006). Synthesis and characterization of an injectable hydrogel with tunable mechanical properties for soft tissue repair. *Biomacromolecules*, *7*(11), 3223–8. doi:10.1021/bm0602536

Hong, Y., Mao, Z., & Wang, H. (2006). Covalently crosslinked chitosan hydrogel formed at neutral pH and body temperature. *Journal of Biomedical Materials Research Part A*, *79A*(4), 913–922. doi:10.1002/jbm.a

Huglin, M. B., Rehab, M. M., & Zakaria, M. B. (1986). Thermodynamic interactions in copolymeric hydrogels. *Macromolecules*, *19*(12), 2986–2991.

Ifkovits, J., Tous, E., Minakawa, M., Morita, M., Robb, J., Koomalsingh, K., … Burdick, J. (2010). Injectable hydrogel properties influence infarct expansion and extent of postinfarction left ventricular remodeling in an ovine model. *Proceedings of the National Academy of Sciences*, *107*(25), 11507–11512.

Jones, D. (2005). HIV facial lipoatrophy: causes and treatment options. *Dermatologic Surgery : Official Publication for American Society for Dermatologic Surgery [et Al.]*, *31*(11 Pt 2), 1519–29; discussion 1529. Retrieved from http://www.ncbi.nlm.nih.gov/pubmed/16416634

Kablik, J., Monheit, G., Yu, L., Chang, G., & Gershkovich, J. (2009). Comparative Physical Properties Of Hyaluronic Acid Dermal Fillers. *Dermatologic Surgery*, *35*, 302–312.

Kadouch, J. a, van Rozelaar, L., Karim, R. B., & Hoekzema, R. (2013). Current treatment methods for combination antiretroviral therapy-induced lipoatrophy of the face. *International Journal of STD & AIDS*, *24*(9), 685–94. doi:10.1177/0956462412474539

Krouskop, T., Wheeler, T., Kallel, F., Garra, B., & Hall, T. (1998). Elastic Moduli of Breast and Prostate Tissues under Compression. *Ultrasonic Imaging*, *20*(4), 260–274.

Levental, I., Georges, P., & Janmey, P. (2007). Soft biological materials and their impact on cell function. *Soft Matter*, *3*(3), 299.

Liu, L., Liu, D., Wang, M., Guocheng, & Chen, J. (2007). Preparation and characterization of sponge-like composites by cross-linking hyaluronic acid and carboxymethylcellulose sodium with adipic dihydrazide. *European Polymer Journal*, *43*(6), 2672–2681.

Marsano, E., Gagliardi, S., Ghioni, F., & Bianchi, E. (2000). Behaviour of gels based on (hydroxypropyl) cellulose methacrylate. *Polymer*, *41*(21), 7691–7698. doi:10.1016/S0032-3861(00)00142-7

Metters, A. T., Anseth, K. S., & Bowman, C. N. (1999). Fundamental studies of biodegradable hydrogels as cartilage replacement materials. *Biomedical Sciences Instrumentation*, *35*, 33–38.

Milani, A. H., Freemont, A. J., Hoyland, J. a, Adlam, D. J., & Saunders, B. R. (2012). Injectable doubly cross-linked microgels for improving the mechanical properties of degenerated intervertebral discs. *Biomacromolecules*, *13*(9), 2793–801. doi:10.1021/bm3007727

Mironi-Harpaz, I., Wang, D. Y., Venkatraman, S., & Seliktar, D. (2012). Photopolymerization of cell-encapsulating hydrogels: Crosslinking efficiency versus cytotoxicity. *Acta Biomaterialia*, *8*(5), 1838–1848.

Monheit, G., & Coleman, K. (2006). Hyaluronic acid fillers. *Dermatologic Therapy*, *19*(3), 141–150.

Narins, R. S., & Bowman, P. H. (2005). Injectable skin fillers. *Clinics in Plastic Surgery*, *32*(2), 151–62. doi:10.1016/j.cps.2004.12.002

Negredo, E., Higueras, C., Adell, X., Martinez, J. C., Martinez, E., Puig, J., … Clotet, B. (2006). Reconstructive treatment for antiretroviral-associated facial lipoatrophy: a prospective study

comparing autologous fat and synthetic substances. *AIDS Patient Care and STDs*, *20*(12), 829–37. doi:10.1089/apc.2006.20.829

Oudshoorn, M., Rissmann, R., Bouwstra, J., & Hennink, W. (2006). Synthesis and characterization of hyperbranched polyglycerol hydrogels. *Biomaterials*, *27*(32), 5471–5479.

Page, J. M., Harmata, A. J., & Guelcher, S. a. (2013). Design and development of reactive injectable and settable polymeric biomaterials. *Journal of Biomedical Materials Research. Part A*, *101*(12), 3630–45. doi:10.1002/jbm.a.34665

Parsons, D. (2006). Carboxymethylcellulose Sodium. In R. C. Rowe, P. J. Sheskey, & S. C. Owen (Eds.), *Handbook of Pharmaceutical Excipients* (5th ed., pp. 120–123). London: Pharmaceutical Press.

Peppas, N. a., Hilt, J. Z., Khademhosseini, a., & Langer, R. (2006). Hydrogels in Biology and Medicine: From Molecular Principles to Bionanotechnology. *Advanced Materials*, *18*(11), 1345–1360. doi:10.1002/adma.200501612

Reeves, R., Ribeiro, A., Lombardo, L., Boyer, R., & Leach, J. B. (2010). Synthesis and Characterization of Carboxymethylcellulose-Methacrylate Hydrogel Cell Scaffolds. *Polymers*, *2*(3), 252–264.

Requena, L., Requena, C., Christensen, L., Zimmermann, U. S., Kutzner, H., & Cerroni, L. (2011). Adverse reactions to injectable soft tissue fillers. *Journal of the American Academy of Dermatology*, *64*(1), 1–34; quiz 35–6. doi:10.1016/j.jaad.2010.02.064

Reza, A. T., & Nicoll, S. B. (2010a). Characterization of novel photocrosslinked carboxymethylcellulose hydrogels for encapsulation of nucleus pulposus cells. *Acta Biomaterialia*, *6*(1), 179–186.

Reza, A. T., & Nicoll, S. B. (2010b). Serum-free, chemically defined medium with TGF-Î² enhances functional properties of nucleus pulposus cell-laden carboxymethylcellulose hydrogel constructs. *Biotechnology and Bioengineering*, *105*(2), 384–395.

Rzany, B., Becker-Wegerich, P., Bachmann, F., Erdmann, R., & Wollina, U. (2009). Hyaluronidase in the correction of hyaluronic acid-based fillers: a review and a recommendation for use. *Journal of Cosmetic Dermatology*, *8*(4), 317–323.

Samani, A., Zubovits, J., & Plewes, D. (2007). Elastic moduli of normal and pathological human breast tissues: an inversion-technique-based investigation of 169 samples. *Physics in Medicine and Biology*, *52*(6), 1565–1576.

Sarkar, N. (1979). Thermal gelation properties of methyl and hydroxypropyl methylcellulose. *J Appl Polym Sci*, *24*, 1073–87.

Shin, H., Temenoff, J., & Mikos, A. (2003). In Vitro Cytotoxicity of Unsaturated Oligo[poly(ethylene glycol) fumarate] Macromers and Their Cross-Linked Hydrogels. *Biomacromolecules*, *4*(3), 552–560.

Shpaisman, N., Sheihet, L., Bushman, J., Winters, J., & Kohn, J. (2012). One-Step Synthesis of Biodegradable Curcumin-Derived Hydrogels as Potential Soft Tissue Fillers after Breast Cancer Surgery. *Biomacromolecules*, *13*(8), 2279–2286.

Slaughter, B. V, Khurshid, S. S., Fisher, O. Z., Khademhosseini, A., & Peppas, N. a. (2009). Hydrogels in regenerative medicine. *Advanced Materials (Deerfield Beach, Fla.)*, *21*(32-33), 3307–29. doi:10.1002/adma.200802106

Smeds, K. A., & Grinstaff, M. W. (2001). Photocrosslinkable polysaccharides for in situ hydrogel formation. *Journal of Biomedical Materials Research*, *54*(1), 115–121.

Stalling, S. S., Akintoye, S. O., & Nicoll, S. B. (2009). Development of photocrosslinked methylcellulose hydrogels for soft tissue reconstruction. *Acta Biomaterialia*, *5*(6), 1911–1918.

Su, W.-Y., Chen, Y.-C., & Lin, F.-H. (2010). Injectable oxidized hyaluronic acid/adipic acid dihydrazide hydrogel for nucleus pulposus regeneration. *Acta Biomaterialia*, *6*(8), 3044–3055.

Suhag, G. S., Bhatnagar, A., & Singh, H. (2008). Poly(hydroxyethyl methacrylate)-based co-polymeric hydrogels for transdermal delivery of salbutamol sulphate. *Journal of Biomaterials Science. Polymer Edition*, *19*(9), 1189–200. doi:10.1163/156856208785540118

Tadros, T. F. (2010). *Rheology of Dispersions: Principles and Applications*. Weinheim, Germany: Wiley-VCH Verlag GmbH & Co. kGaA;

Temenoff, J., Shin, H., Conway, D., Engel, P., & Mikos, A. (2003). In Vitro Cytotoxicity of Redox Radical Initiators for Cross-Linking of Oligo(poly(ethylene glycol) fumarate) Macromers. *Biomacromolecules*, *4*(6), 1605–1613.

Van Tomme, S. R., Storm, G., & Hennink, W. E. (2008). In situ gelling hydrogels for pharmaceutical and biomedical applications. *International Journal of Pharmaceutics*, *355*(1-2), 1–18. doi:10.1016/j.ijpharm.2008.01.057

Varma, D., Gold, G. T., Taub, P. J., & Nicoll, S. B. (2014). Injectable Carboxymethylcellulose Hydrogels for Soft Tissue Filler Applications. *Acta Biomaterialia*, (August). doi:10.1016/j.actbio.2014.08.013

Weissleder, R. (2001). A clearer vision for in vivo imaging. *Nature Biotechnology*, *19*(4), 316–317.

668 Winter, H. H., & Chambon, F. (1986). Analysis of linear viscoelasticity of a crosslinking
669 polymer at the gel point. *Journal of Rheology*, *30*(2), 367–382.

670 Yang, H., Zheng, Y., Zhao, B., Shao, T., Shi, Q., Zhou, N., & Cai, W. (2013). Encapsulation of
671 liver microsomes into a thermosensitive hydrogel for characterization of drug metabolism
672 and toxicity. *Biomaterials*, *34*(38), 9770–8. doi:10.1016/j.biomaterials.2013.09.025

673

674

Figure legends

Fig. 1. Schematic of methacrylated MC synthesis and hydrogel fabrication using ammonium persulfate and ascorbic acid redox initiators.

Fig. 2. Representative ^{1}H-NMR spectra of (A) modified MC indicating peaks associated with the methacrylate groups on the MC polymer backbone, and of (B) a crosslinked MC hydrogel. R1 represents the methylene protons and R2 corresponds to the methyl protons of the methacrylate group.

Fig. 3. Representative transmission FTIR spectra of the MC base polymer, methacrylated MC polymer, and the lyophilized $MC_{4\%}$ hydrogel. Black arrows indicate characteristic peaks of MC and methacrylate groups referenced in the text.

Fig. 4. Equilibrium mechanical properties of MC hydrogels as a function of macromer concentration. (A) Equilibrium Young's modulus, E_y and (B) peak stress, σ_{pk}. Significance set at $p < 0.05$: *, significantly different with respect to all other groups.

Fig. 5. Representative graphs of the evolution of rheological properties during the redox-polymerization of $MC_{2\%}$ (A, B) and $MC_{4\%}$ (C, D). (A, C) Gelation onset, defined as $G'/G''=1$, is indicated by the arrow. The phase shift, δ (right axis), is also shown. (B,D) Gelation completion, defined as the first time at which there were at least four consecutive points with less than 2% change in G', is indicated by the vertical line. The concurrent evolution of G'' is also graphed, and the x-axes of the vertical panels are aligned to allow for direct comparison between curves.

Fig. 6. Enzymatic degradation assessment. Representative stereomicrographs of $MC_{4\%}$ constructs (A) 0, (B) 4, and (C) 16 hours after cellulase treatment. Complete degradation was observed by 24 hours. Scale is in mm. (D) Wet weight of $MC_{4\%}$ hydrogels as a function of exposure time to cellulase. Significance set at $p < 0.05$: #, significant relative to 0 and 4 hours.

Fig. 7. Cell viability analysis. Representative Live/Dead fluorescent images of fibroblasts following 4 days of co-culture (A) without (control), (B) with $MC_{2\%}$, and (C) with $MC_{4\%}$ hydrogels. Live cells are stained green (with calcein AM) and dead cells are shown in red (with ethidium homodimer). Scale bar = 50 μm. (D) DNA content of fibroblasts co-cultured with $MC_{2\%}$ and $MC_{4\%}$ hydrogels. Significance set at $p < 0.05$: No statistical difference relative to the control of the corresponding day.

Fig. 8. Mechanical Stability. (A) The E_y values of $MC_{4\%}$ constructs measured over 12 weeks. Significance set at $p < 0.05$: there was no statistical difference among the time points. Stereomicrographs of representative gels at (B) 1, (C) 4, (D) 8, and (E) 12 weeks after initial casting. Scale is in mm.

Table 1

Macromer concentration	Q_w	v_e *(mol/cm^3)*	ξ *(nm)*
2%	56.10 ± 1.94 [a]	1.43E-05 ± 8.24E-07 [a]	76.38 ± 2.94 [a]
3%	38.55 ± 2.35 [a]	2.61E-05 ± 2.59E-06 [a]	50.45 ± 3.36 [a]
4%	33.19 ± 0.79 [a]	3.27E-05 ± 1.21E-06 [a]	42.86 ± 1.11 [a]

Table 1. Swelling ratio and related physical properties of MC hydrogels. Equilibrium weight swelling ratio, Q_w; effective crosslinking density, v_e; and hydrogel mesh size, ξ. Significance set at $p < 0.05$: [a] significantly different with respect to all other groups.

Table 2

	Macromer Concentration (w/v)	Time (min)	*G'* (Pa)	*G''* (Pa)	δ	$\lvert\eta^*\rvert$ (Pa·s)
Gelation Onset	2%	1.58 ± 0.67 [a]	1.93 ± 1.87 [a]	0.80 ± 0.68 [b]	28.28 ± 13.52 [a,b]	0.35 ± 0.30 [a]
	4%	2.25 ± 1.02 [a]	2.73 ± 1.92 [a]	2.50 ± 2.16 [a,b]	39.04 ± 7.65 [b]	0.59 ± 0.46 [a]
Gelation Completion	2%	21.03 ± 1.70 [a,b]	245.3 ± 52.72 [a,b]	2.70 ± 0.98 [b]	0.66 ± 0.26 [a,b]	39.11 ± 8.43 [a,b]
	4%	15.02 ± 0.54 [a,b]	937.9 ± 322.8 [a,b]	9.29 ± 1.04 [a,b]	0.61 ± 0.17	149.2 ± 51.3 [a,b]

Table 2. Gelation/rheological properties of redox-polymerized $MC_{2\%}$ and $MC_{4\%}$ hydrogels. Storage modulus, G'; Loss modulus, G''; the phase angle, δ; complex viscosity, $\lvert\eta^*\rvert$. Significance set at $p < 0.05$: [a], significantly different from other gelation time within macromer concentration; [b], significantly different from other macromer concentration within gelation time.